Available online at www.CivileJournal.org

Civil Engineering Journal

(E-ISSN: 2476-3055; ISSN: 2676-6957)

Vol. 10, Special Issue, 2024
"Sustainable Infrastructure and Structural Engineering:
Innovations in Construction and Design"

Role of Slag Replacement on Strength Enhancement of One-Part High-Calcium Fly Ash Geopolymer

Darrakorn Intarabut [1], Piti Sukontasukkul [2*], Tanakorn Phoo-ngernkham [3], Sakonwan Hanjitsuwan [4], Vanchai Sata [5], Poopatai Chumpol [2], Worathep Sae-Long [6], Hexin Zhang [7], Prinya Chindaprasirt [5, 8]

[1] *Department of Civil Engineering, Faculty of Engineering, Rajamangala University of Technology Phra Nakhon, Bangkok, Thailand.*

[2] *Construction and Building Materials Research Center, Department of Civil Engineering, King Mongkut's University of Technology North Bangkok, Bangkok 10800, Thailand.*

[3] *Sustainable Construction Material Technology Research Unit, Department of Civil Engineering, Faculty of Engineering and Technology, Rajamangala University of Technology Isan, Nakhon Ratchasima 30000, Thailand.*

[4] *Department of Survey and Geomatics Engineering, Faculty of Engineering and Technology, Rajamangala University of Technology Isan, Nakhon Ratchasima 30000, Thailand.*

[5] *Sustainable Infrastructure Research and Development Center, Department of Civil Engineering, Faculty of Engineering, Khon Kaen University, Khon Kaen 40002, Thailand.*

[6] *Department of Civil Engineering, Faculty of Engineering, Phayao University, Phayao 56000, Thailand.*

[7] *School of Computing, Engineering and the Built Environment, Edinburgh Napier University, Edinburgh EH10 5DT, Scotland, United Kingdom.*

[8] *Academy of Science, Royal Society of Thailand, Dusit, Bangkok 10300, Thailand.*

Received 26 June 2024; Revised 13 November 2024; Accepted 25 November 2024; Published 16 December 2024

Abstract

This paper reports the effect of slag (SL) replacement and water-to-binder (w/b) ratio on properties of one-part geopolymer derived from high-calcium fly ash (FA) and sodium silicate powder (NP). The FA was replaced by SL at the rates of 20% and 40%, respectively. This study focused on conducting experimental tests to evaluate the relative slump, setting time, compressive strength, and flexural strength of one-part FA-based geopolymer. The relationship between compressive and flexural strengths of one-part geopolymer mortar was expressed using the simplified linear regression model, whereas the normalization of compressive and flexural strengths with SL replacement by the strength of one-part geopolymer mortar without SL as the divisor was also evaluated. Experimental results showed that the increase of SL replacement and w/b ratio significantly affected the workability and strength development of one-part geopolymer mortar. Higher SL replacement exhibited a positive effect on their compressive and flexural strengths; however, a reduction in its setting time was obtained. The enhancement in strength development of one-part geopolymer was primarily due to the increased calcium content of SL. Similarly, reducing the w/b ratio in the production of one-part geopolymer resulted in a decrease in setting time and an increase in strength development. Based on the relationship between compressive and flexural strengths, the prediction coefficient value (R^2) obtained from the curve fitting procedure was 0.835, indicating a good level of reliability and acceptability for engineering applications.

Keywords: One-Part Geopolymer; Slag Replacement; Strength Development; Fly Ash Based Geopolymer.

* Corresponding author: piti.s@eng.kmutnb.ac.th

http://dx.doi.org/10.28991/CEJ-SP2024-010-013

1. Introduction

Conventional or two-part geopolymer (Geopolymer) refers to a type of geopolymer system that consists of two separate components: a binder and an activator solution. The geopolymer binder typically consists of dry powder containing precursor materials such as fly ash (FA), slag, or other aluminosilicate materials. The binder acts as the reactive component that undergoes geopolymerization when activated [1, 2]. The activator solution, on the other hand, is a liquid containing alkaline or alkaline-earth metal hydroxides, silicates, or other alkaline activators [3, 4]. When mixed with the binder, this solution initiates the geopolymerization reaction, forming the geopolymer matrix [3, 5-8].

Geopolymers can be classified into three types based on their calcium content [9, 10]: (a) High-calcium systems, which produce calcium silicate hydrate (C-S-H) and/or calcium aluminosilicate hydrate (C-A-S-H) gels that coexist with sodium aluminosilicate hydrate (N-A-S-H) gels as hybrid C-(N)-A-S-H gels, (b) Low-calcium systems, which mainly form N-A-S-H gel, and (c) Mixed systems, which combine high- and low-calcium materials, sometimes with Portland cement (PC). Detphan et al. [11] and Phoo-ngernkham et al. [12] demonstrated that the hybrid C-(N)-A-S-H gels from high-calcium systems can enhance the compressive and bond strengths of geopolymer system when cured at ambient temperature.

However, handling alkali solutions in the field presents challenges in terms of safety and practicality. The highly alkaline nature of these solutions poses risks such as irritation, burns, blindness, or esophageal perforation upon contact [13, 14]. To mitigate these risks, the use of personal protective equipment (PPE) and strict adherence to safety protocols are essential. Furthermore, an alternative approach to minimize direct handling of these hazardous solutions is the development of one-part geopolymer systems.

One-part geopolymer systems simplify the process by requiring only the addition of water to a dry powder or pre-mixed liquid to produce a solid material [15-19]. This approach offers numerous advantages over the two-part systems, including environmental sustainability, ease of use, and cost-effectiveness, as it reduces the complexity and risk of errors during mixing.

Several researchers have explored the characteristics of one-part geopolymers. For example, Tesanasin et al. [15] demonstrated that stabilizing marginal lateritic soil with one-part high-calcium FA geopolymer improved the engineering properties of pavement materials. Similarly, Phiangphimai et al. [16, 17] found that a dry powder mixture of GEOPOLYMER and Portland cement (PC) activated with tap water and sodium hydroxide flakes improved bond strength and durability when used as a coating material for concrete structures.

Despite its advantages, one-part geopolymer systems present some challenges, such as limited control over curing time, reduced storage life, slower strength development, and lower mechanical properties. The slower strength development is often attributed to the powdered alkali activators, particularly sodium silicate, which can be difficult to dissolve uniformly during mixing. This results in non-uniform geopolymerization and hampers strength development. For instance, Liew et al. [20] reported low strength in one-part geopolymer prepared from kaolin-derived geopolymer powder and alkaline solutions. Feng et al. [21] also found that one-part geopolymer made with sodium hydroxide solution had higher compressive strength than that made with sodium carbonate powder at the same dosage.

To address these issues, several researchers have explored various factors influencing strength development in one-part geopolymer systems, with raw material selection being a critical factor. For example, Phiangphimai et al. [16, 17] used a mixture of geopolymer and PC, activated by sodium hydroxide flakes and tap water, to achieve a bond strength of 33 MPa. Hajimohammadi & Deventer [22] optimized the curing conditions and adjusted the silica/aluminum ratio in their study of one-part FA-based geopolymers, achieving a compressive strength of 65 MPa. Similarly, Sturm et al. [23] examined the effects of heat treatment on one-part geopolymer-zeolite composites, reaching compressive strengths of 28 MPa at temperatures between 200°C and 400°C. However, high-temperature curing can introduce complexities, increase costs, and potentially lower long-term strength in practical applications. Mohamed et al. [24] also demonstrated that increasing the alkali content in one-part geopolymer made from high-calcium FA significantly improved compressive strength, reaching 50 MPa. Additionally, Nematollahi et al. [25] achieved compressive strengths exceeding 37 MPa by using low-calcium FA, slag, and hydrated lime, activated by sodium silicate and sodium hydroxide powders.

Despite advancements, one-part geopolymers still struggle to achieve high compressive strengths, especially under ambient curing conditions. Enhancing strength typically requires methods such as increasing curing temperatures, adjusting alkali content, or combining multiple activators. However, these methods introduce additional challenges related to cost, complexity, and long-term performance.

1.1. Research Gap

While extensive research has been conducted on fly ash (FA) and slag-based geopolymer systems, most studies focus on two-part geopolymers [26-30]. Research on one-part geopolymers, especially those made from FA and slag, remains limited. For instance, Yousefi Oderji et al. [31] studied one-part FA-based geopolymers with slag and various activators, finding that slag improved strength but reduced workability. Chen et al. [32] also investigated the mechanical properties of one-part geopolymers made from coal gasification slag using alkali fusion and additive methods.

1.2. Research Objective

This study aims to explore the potential of one-part geopolymer systems using high-calcium fly ash and ground blast furnace slag (GBFS) as sustainable construction materials. The high calcium oxide content in FA and GBFS (27.8% and 36.7%, respectively) is known to accelerate early strength development in geopolymers. By utilizing these materials, which are rich in calcium oxide, silica, and alumina—key elements for strength development—this research seeks to improve the mechanical properties of one-part geopolymers, even under ambient temperature curing, without increasing the number or complexity of alkali activators (see Table 1).

Table 1. Chemical composition of silica fume and slag

Materials	SiO_2	Al_2O_3	Fe_2O_3	CaO	MgO	Na_2O	K_2O	SO_3	LOI
FA (%)	31.9	15.9	14.1	27.8	3.7	1.9	1.9	2.5	0.2
SL (%)	32.3	15.4	0.6	36.7	7.2	0.7	0.4	1.2	0.7

2. Research Methodology

2.1. Materials

In this study, three components: high-calcium fly ash (FA), slag (SL), and sodium silicate powder (NP) were used as the starting materials for the production of one-part FA-based geopolymer. Table 1 lists the chemical compositions of FA and SL. FA with average particle size of 16.4 µm and specific gravity of 2.61, contained a combined SiO_2+Al_2O_3+Fe_2O_3 content of 61.80%. However, due to its high CaO content; thus this FA was Class C as described in ASTM C618-22 [33]. SL had a specific gravity of 2.91, an average particle size of 6.4 µm, and a combined SiO_2+Al_2O_3+Fe_2O_3 content of 48.30%, with CaO of 37%. The sodium silicate powder (NP) used in the study had a specific gravity of 0.95 and silica modulus (SiO_2/Na_2O molar ratio) of 1.0. Several publications [34, 35] reported that the FA-SL-based GEOPOLYMER with SiO_2/Na_2O molar ratios between 0.5 and 1.0 exhibited positive mechanical properties. As for the fine aggregate, river sand was employed, which possesses a specific gravity of 2.60 and a fineness modulus of 2.85. Granular diagram is shown in Figure 1.

Figure 1. Granular diagram

2.2. Mix Proportions

The control one-part geopolymer mortar consisted of four components: FA, NP, fine aggregate, and tap water. To examine the impact of SL, the FA was substituted with SL at weight percentages of 20% and 40%, respectively. In addition, to study the influence of the water/binder (w/b) ratio, three w/b ratios were considered at 0.25, 0.30, and 0.35, respectively. The ratio between the fine aggregate and binder was set constant at 1.25, which was based on the previous studies [19, 28]. The detail mix proportions of one-part FA-based geopolymer were summarized in Table 2.

Table 2. Mix proportions of one-part FA-based geopolymer mortar (kg/m^3)

No.	Symbol	w/b ratio	Fly ash (kg)	Sodium Silicate (kg)	Slag (kg)	River sand (kg)	Tap water (kg)
1	0.25/F9/N1/S0	0.25	789	88	-	1096	219
2	0.25/F7/N1/S2		618	88	177	1103	221
3	0.25/F5/N1/S4		444	88	355	1111	222
4	0.30/F9/N1/S0	0.30	756	84	-	1050	252
5	0.30/F7/N1/S2		592	85	169	1057	254
6	0.30/F5/N1/S4		425	85	340	1064	255
7	0.35/F9/N1/S0	0.35	725	81	-	1008	282
8	0.35/F7/N1/S2		568	81	162	1014	284
9	0.35/F5/N1/S4		408	82	326	1020	286

2.3. Specimen Preparation

The preparation process began by mixing all solid ingredients in a pan mixer for 2 minutes. Afterwards, tap water was added, and the mixing continued for an additional 2 minutes. The fresh mixes were then poured into molds in 2-3 layers, depending on the specimen type. Each layer was compacted using a steel rod, applying 25 repetitions. After finish preparing, the specimens were covered with plastic sheet for 24 hours at room temperature, demolded, wrapped with plastic sheet and cured in a controlled temperature of 25ºC for 28 days.

2.4. Experimental Series

2.4.1. Mini Slump Test

Briefly, the test begins by taking a small amount of fresh one-part geopolymer mortar and ensuring it is well-mixed and free from lumps or air pockets. Then, place the mini slump cone on a flat, clean surface and moisten the inside of the cone with water to prevent sticking. Carefully fill the cone with fresh mortar, ensuring it is evenly distributed and compacted in each layer using a tamper. Hold the mold firmly and lift it vertically, steadily, and smoothly, without any twisting or lateral movement. After lifting the cone, allow the fresh mortar to flow for 1 minutes and measure the diameter using a ruler or calipers (Figure 2). Take at least two measurements perpendicular to each other and use the average value to determine the relative slump using Equation 1.

$$D_r = \left(\frac{\mathrm{D}}{D_0}\right)^2 - 100 \quad (1)$$

where D_r is the relative slump, D is the average diameter of the spread geopolymer (mm), and D_0 is the diameter of slump cone (mm).

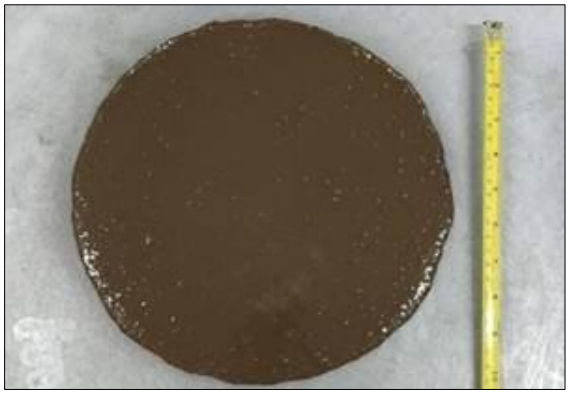

Figure 2. Mini slump test

2.4.2. Setting Time Test

The measurement of setting time value of one-part geopolymer paste was tested as described in ASTM C191-13 [36] using a Vicat apparatus. The test process begins with mixing the fresh mortar according to the procedure described in section 2.3. Then, place the Vicat apparatus on a clean and stable surface. Fill the mold with the prepared fresh mortar,

ensuring it is evenly distributed. Lower the Vicat needle gently into the center of the paste, making sure it makes contact with the top surface of the paste. Release the needle and allow it to penetrate and remain in the paste. The initial setting time is the duration from the start of mixing until the paste begins to lose its plasticity and resists penetration by the Vicat needle. This is indicated when the needle can penetrate the paste by 25 mm. The final setting time is the period when the paste has completely lost its plasticity and the Vicat needle is unable to penetrate the paste. Instead, the needle only creates a visible impression on the surface of the paste.

2.4.3. Compression Test

The compression test was conducted following the guidelines outlined in ASTM C109 [37]. The one-part geopolymer mortars were prepared in the form of cubes with dimensions of 50x50x50 mm and cured under controlled conditions as described in section 2.3. After the curing period, the specimens were removed from the curing environment and subjected to testing using a universal testing machine. A gradually increasing load was applied until failure occurred (Figure 3-a). The maximum load at failure was recorded, and the compressive strength was calculated by dividing the maximum load by the cross-sectional area of the specimen.

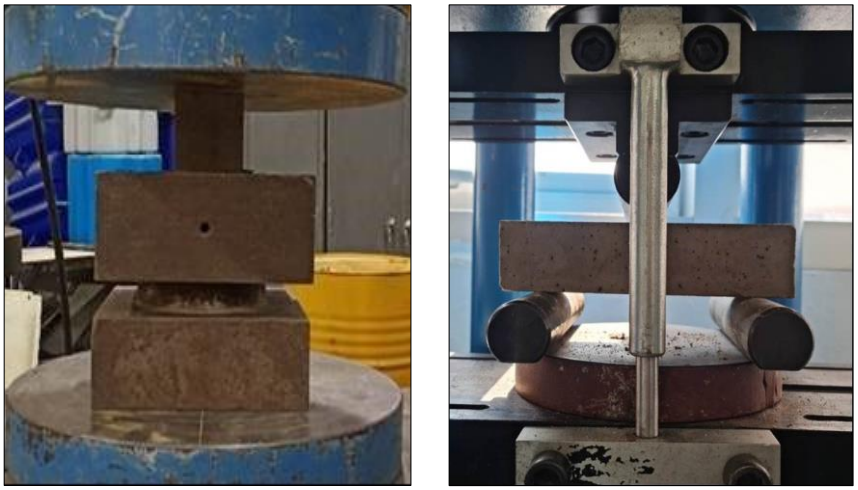

(a) (b)

Figure 3. (a) Compression test and (b) Flexural test

2.4.4. Flexural Strength Test

The flexural test was carried out following the guidelines in ASTM C348-21 [38]. The one-part geopolymer mortars were prepared in the form of prism with dimensions of 50×50×150 mm and cured under the controlled condition as described in section 2.3. At the specified age, the specimens were removed from the curing environment and tested using a universal testing machine. The specimens were subjected to a three-point bending test with load acting at the center of the prism (Figure 3-b). The load was gradually increased until the specimen fractured. Using the recorded maximum load, the modulus of rupture can be calculated using Equation 2.

$$\sigma = \frac{3FL}{2bd^2} \quad (2)$$

where F is the maximum load (N), L is the clear span length (mm), b is the specimen height (mm), and d is the specimen width (mm).

2.5. Life Cycle Assessment (LCA)

In addition to the experimental series conducted in this study to evaluate the properties of one-part geopolymer, a Life Cycle Assessment (LCA) was also performed. However, the scope of the LCA is limited to the manufacturing phase of the one-part geopolymer materials. This focus was chosen to ensure consistency in the analysis, as other life cycle stages, such as transportation and storage, can vary significantly based on factors such as transportation distance, modes of transport, and local storage practices. By isolating the manufacturing process, we can provide a more reliable and comparable assessment of the environmental impact associated with the production of the geopolymer materials themselves. Our focus within the environmental impact category is on energy consumption during production, which is then converted to Global Warming Potential (GWP), expressed in kilograms of CO_2 equivalents.

The experimental process is summarized and illustrated in Figure 4.

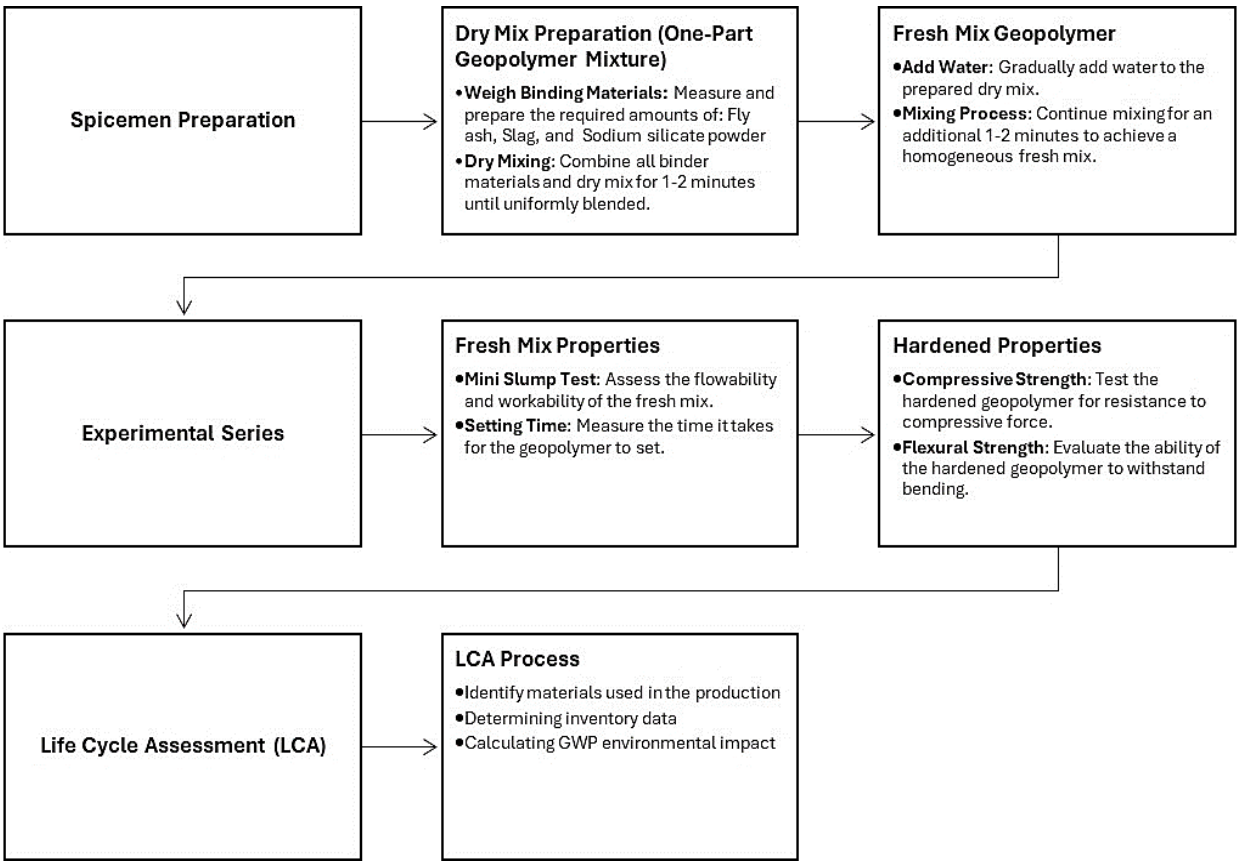

Figure 4. Experimental process

3. Results and discussion

3.1. Relative Slump

The relative slump test results of the one-part fly ash (FA)-based geopolymer mortar, as illustrated in Figure 5, clearly demonstrate that the water-to-binder (w/b) ratio has a significant effect on the workability and flowability of the mixtures.

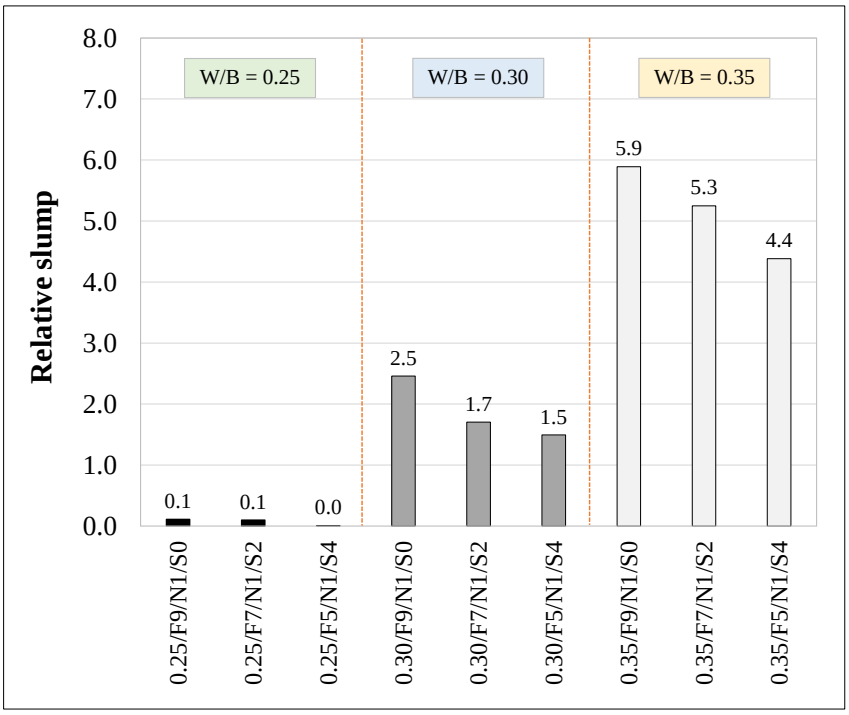

Figure 5. Relative slump value of one-part geopolymer mortar

At a w/b ratio of 0.25, the slump values were consistently low across all slag replacement rates (S0, S2, and S4), ranging from 0.0 to 0.1. This indicates extremely poor workability and flowability of the one-part geopolymer mortar at this low water content. The lack of sufficient free water limits the lubrication between particles, leading to higher internal friction and, consequently, a more rigid and less workable mixture. Low w/b ratios often result in a compacted mix where particles are too close to move freely, reducing mobility and resulting in negligible slump values. This is consistent with the common behavior in cementitious systems where low water content leads to lower workability.

As the w/b ratio was increased to 0.30, the slump values significantly improved, ranging from 1.5 to 2.5. This increase in slump suggests enhanced workability and flowability, likely due to the additional water that reduces internal friction, allowing particles to slide past each other more easily. The increased water content provides better wetting of the dry particles, improving the mix's ability to deform under its own weight and flow more freely.

Further increasing the w/b ratio to 0.35 led to a more pronounced improvement in slump values, which ranged from 4.4 to 5.9. This continued increase in workability can be attributed to the higher fluidity provided by the increased water content. The results align with findings from Sinsiri et al. [4], who suggested that a higher w/b ratio reduces particle interaction and friction within the geopolymer matrix, thus improving workability.

In addition to the w/b ratio, the slag (SL) replacement rate also had a noticeable influence on the workability of the one-part geopolymer mixtures. At each w/b ratio, an increase in SL replacement rate generally resulted in a decrease in slump values, indicating reduced workability. For instance, at a w/b ratio of 0.35, the relative slump values decreased from 5.9 (S0) to 5.3 (S2) and further to 4.4 (S4) as the SL replacement rate increased from 0% to 40%. This reduction in workability with higher slag content may be attributed to several factors:

1. Smaller particle size of slag: The finer particles of slag (as described in Section 2.3) have a higher specific surface area, which increases the water demand to wet the surface adequately. When the water content is fixed or relatively low, this leads to a stiffer mixture with reduced workability. This phenomenon is consistent with similar findings in cementitious materials where finer particles reduce flowability due to their increased surface area.
2. Particle shape: The angular shape of the slag particles, as reported by Phoo-ngernkham et al. [27] and Sukontasukkul et al. [28], may also contribute to the reduction in workability. Angular particles increase internal friction and resistance to flow compared to spherical particles, which move past each other more easily. This added friction from the angular slag particles makes it more difficult for the mixture to flow, reducing the slump.

3.2. Setting Time

The setting behavior of one-part fly ash (FA)-based geopolymer paste with varying water-to-binder (w/b) ratios and slag (SL) replacement levels was evaluated, with both the initial and final setting times recorded. The results of these tests are shown in Figure 6.

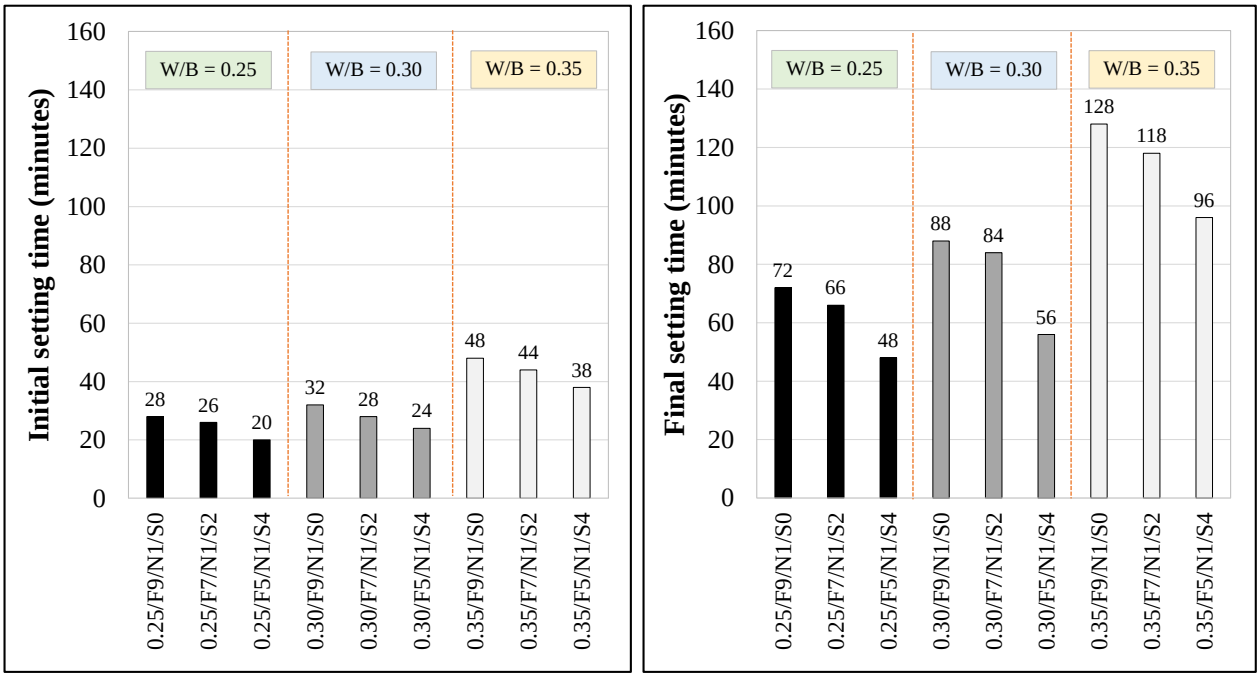

(a) Initial setting time (b) Final setting time

Figure 6. Setting time of one-part geopolymer paste

3.2.1. Influence of Water-to-Binder Ratio

The results clearly indicate that the w/b ratio plays a critical role in determining the setting time of the one-part geopolymer paste, similar to its influence on the setting time of conventional Portland cement (PC) pastes [17].

- At a w/b ratio of 0.25, the geopolymer paste exhibited relatively short initial setting times, ranging from 20 to 28 minutes. The final setting time was also quick, ranging from 48 to 72 minutes. This rapid setting behavior at lower w/b ratios is likely due to the limited amount of free water, which leads to faster formation of the aluminosilicate network and accelerates the overall geopolymerization process.
- Increasing the w/b ratio to 0.30 extended the initial setting time to between 24 and 32 minutes, while the final setting time increased to between 56 and 88 minutes. The increase in setting time with higher w/b ratios can be attributed to the dilution effect caused by the additional water, which slows down the reaction kinetics and delays the formation of a stable geopolymer matrix.
- At the highest w/b ratio of 0.35, the setting times were the longest, with initial setting times between 38 and 48 minutes, and final setting times between 96 and 128 minutes. The extended setting times at higher w/b ratios are consistent with the behavior of conventional cementitious materials, where increased water content leads to delayed setting due to reduced particle-particle interaction and slower reaction rates.

These results agree with the findings of previous studies, such as Sinsiri et al. [4], where higher w/b ratios were shown to reduce particle interaction within the geopolymer matrix, contributing to a delay in setting.

3.2.2. Influence of Slag Replacement (SL)

The addition of slag (SL) as a partial replacement for FA also significantly influenced the setting time of the one-part geopolymer paste. As the proportion of SL increased, the setting times consistently decreased.

- At a w/b ratio of 0.25, increasing the SL replacement rate from 0% to 40% reduced the initial setting time from 28 minutes to 20 minutes, while the final setting time decreased from 72 minutes to 48 minutes.
- Similarly, at a w/b ratio of 0.35, the initial setting time decreased from 48 minutes (S0) to 38 minutes (S4), and the final setting time dropped from 128 minutes (S0) to 96 minutes (S4).

This reduction in setting time with increasing SL content can be attributed to the higher calcium oxide (CaO) content in SL compared to FA. It is well-known that the setting time of geopolymer system is partly controlled by the amount of CaO in the system [39-42]. The SL used in this study contained approximately 25% more CaO than FA, and as the SL replacement rate increased from 0% to 40%, the CaO content in the system rose by approximately 6.40% to 12.85%, respectively. The presence of additional CaO accelerates the reaction between calcium and silicate species, forming calcium silicate hydrate (C-S-H) gel, which contributes to faster setting.

This trend is well-documented in the literature. Vikas & Rao [43] demonstrated a marked reduction in setting time when replacing FA with SL at varying levels, with a decrease in setting time from over 24 hours (100% FA) to just 41 minutes at 30% SL replacement. Similarly, Yousefi Oderji et al. [31] observed a reduction in initial setting time from 170 minutes to just 30 minutes when ground granulated blast furnace slag (GGBS) was used to replace FA at 15% by weight. This is primarily due to the higher CaO content in SL and GGBS, which enhances the geopolymerization process [44]. Another factor influencing the setting time is the particle size of the slag used in this study. The finer particle size of the SL increases the surface area available for reaction, which can lead to faster hydration and setting. Moreover, the angular shape of the SL particles (as noted by Phoo-ngernkham et al. [27] and Sukontasukkul et al. [28]) increases the water demand of the system, further influencing the setting behavior.

3.3. Mechanical Properties

3.3.1. Effect of Slag Replacement Ratio

3.3.1.1. Compressive Strength

The results demonstrate that the replacement of fly ash (FA) with slag (SL) significantly enhances the compressive strength of one-part FA-based geopolymer mortars, as illustrated in Figure 7-a. The compressive strength of the geopolymer mortar increased notably with increasing SL content across all water-to-binder (w/b) ratios.

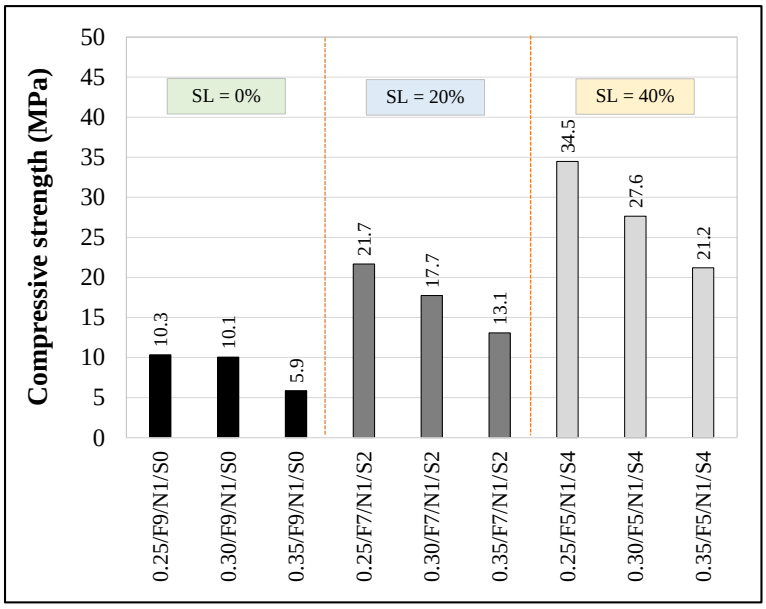

(a)

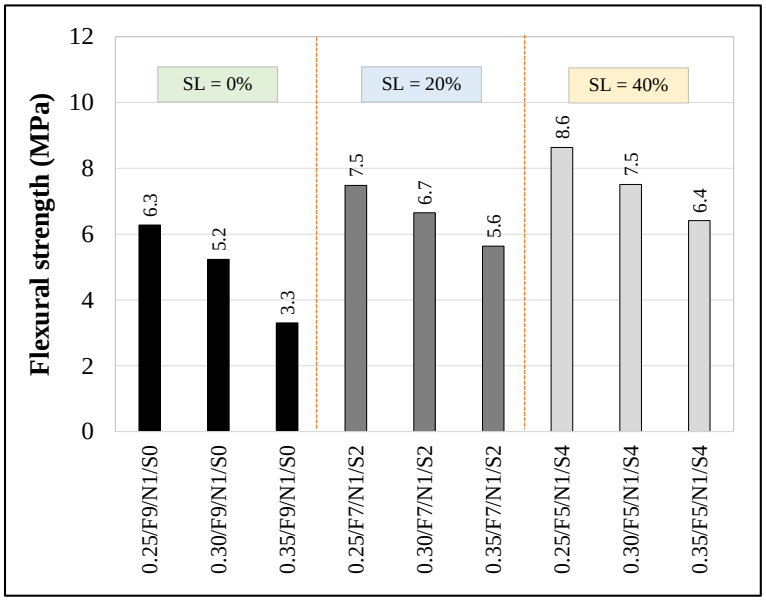

(b)

Figure 7. Effect of slag replacement rates on (a) compressive and (b) flexural strengths

- Without slag (S0), the compressive strength ranged from 5.9 MPa to 10.3 MPa, depending on the w/b ratio. This relatively low strength is due to the FA's lower calcium content, which limits the formation of calcium silicate hydrate (C-S-H) gels, a key component that contributes to mechanical strength.
- At 40% SL replacement (S4), the 28-day compressive strength increased dramatically, reaching values between 21.2 MPa to 34.5 MPa, representing an increase of 76% to 262%. The significant improvement in compressive strength can be attributed to the higher calcium content of SL, which promotes the formation of hybrid C-(N)-A-S-H gels alongside the conventional N-A-S-H gels in the geopolymer matrix. Calcium ions from SL react with $SiO_{□}$ and $Al_{□}O_{□}$ from FA and SL to produce additional C-S-H phases that densify the microstructure, as reported in several studies [12, 45, 46].

This finding is consistent with the work of Yip et al. [47], who showed that the addition of ground granulated blast-furnace slag (GGBS), which has a high CaO content, to metakaolin-based geopolymer systems resulted in the formation of C-S-H gels, in addition to N-A-S-H gels. This produced a denser paste microstructure and led to a marked increase in compressive strength.

Additionally, the work of Phoo-ngernkham et al. [27] supports these observations, as they demonstrated extremely high compressive and shear bond strengths in geopolymer pastes made with GBFS activated by sodium silicate solution. The presence of amorphous reaction products, with only small amounts of crystalline C-S-H, contributed to these high strengths, which were confirmed by XRD analysis.

3.3.1.2. Flexural Strength

A similar trend was observed for flexural strength, as illustrated in Figure 7-b. As the SL content increased, the flexural strength also improved:

- For instance, at a w/b ratio of 0.25, the flexural strength increased from 6.3 MPa (S0) to 8.6 MPa (S4) when the SL replacement reached 40%.
- The increase in flexural strength was also observed for w/b ratios of 0.30 and 0.35, although the magnitude of the increase was smaller compared to compressive strength, ranging from 19% to 94%.

The improvement in flexural strength can also be linked to the enhanced formation of C-S-H gels, which increase the overall stiffness and resistance to bending forces. However, the flexural strength increase was not as substantial as that of compressive strength. This could be due to the nature of geopolymer mortar, where compressive strength benefits more significantly from densification of the matrix, while flexural strength improvements depend on the development of a cohesive and continuous matrix across tensile zones.

3.3.2. Effect of Slag Replacement Ratio

3.3.2.1 Compressive Strength

The compressive strength of one-part FA-based geopolymer mortar is also influenced by the w/b ratio. As shown in Figure 8-a, increasing the w/b ratio from 0.25 to 0.35 results in a general decrease in compressive strength.

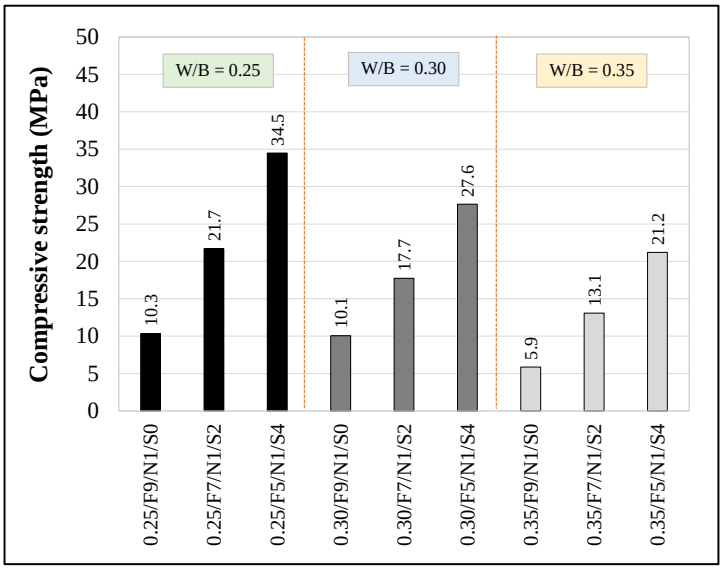

(a)

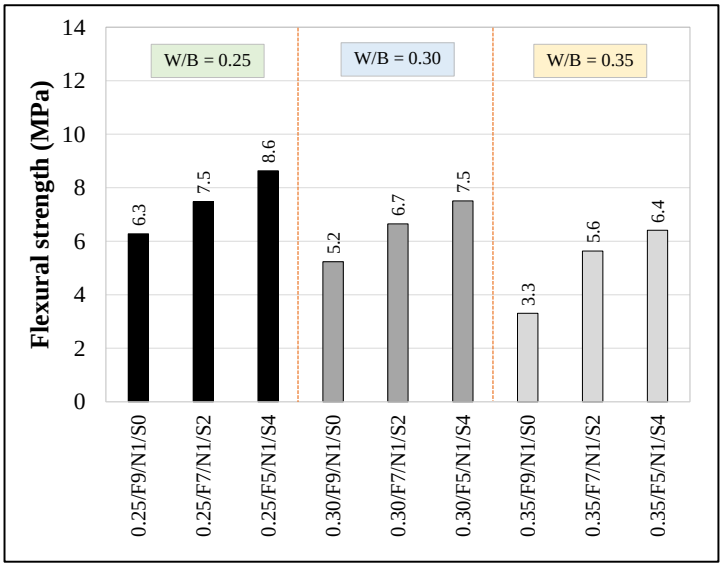

(b)

Figure 8. Effect of w/b ratios on (a) compressive and (b) flexural strengths of one-part geopolymer mortar

- At a w/b ratio of 0.25, the compressive strength ranged from 10.35 MPa (S0) to 34.48 MPa (S4), depending on the slag content. This is the highest strength recorded across the w/b ratios tested, indicating that a low w/b ratio enhances the polymerization process, leading to a denser matrix with fewer voids.
- Increasing the w/b ratio to 0.30 resulted in a slight reduction in compressive strength, with values ranging from 10.06 MPa (S0) to 27.64 MPa (S4). This reduction can be attributed to the additional free water, which dilutes the binder content, slows the polymerization process, and results in more unreacted particles remaining in the matrix.
- Further increasing the w/b ratio to 0.35 led to a significant decrease in compressive strength, ranging from 5.86 MPa (S0) to 21.19 MPa (S4), which represents a reduction of 39% to 43% compared to the 0.25 w/b ratio. The excessive water content at this ratio increases the amount of residual, unreacted water in the system. Once this water evaporates, it creates voids in the matrix, weakening the structure and reducing both compressive and flexural strength.

These findings are in line with those of previous studies [4, 48], which noted that increasing the w/b ratio leads to more air voids in the geopolymer matrix after polymerization, negatively impacting strength.

3.3.2.2. Flexural Strength

Similar to the trend observed for compressive strength, the flexural strength of the one-part FA-based geopolymer mortar decreased as the w/b ratio increased, as illustrated in Figure 8b.

- At a w/b ratio of 0.25, the flexural strength values were 6.3 MPa (S0), 7.5 MPa (S2), and 8.6 MPa (S4), depending on the SL content.
- As the w/b ratio increased to 0.35, the flexural strength decreased to 3.3 MPa (S0), 5.6 MPa (S2), and 6.4 MPa (S4).

The reduction in flexural strength with increasing w/b ratios is a result of the same mechanism affecting compressive strength—an increase in air voids within the matrix due to unreacted water. These voids act as weak points in the matrix, reducing its ability to withstand tensile forces during flexure.

3.4. Relationship between Compressive and Flexural Strengths

Figure 9 illustrates the normalization of compressive strength for varying slag (SL) replacement ratios, relative to the compressive strength of one-part geopolymer mortar without SL (i.e., at 0% SL replacement). The relationship was modeled using an exponential function, with the 28-day compressive strength of the control mix (0% SL) serving as the baseline. This approach is consistent with the methods frequently applied to cementitious materials in prior studies [41, 49]. Equation 3 provides an empirical expression that approximates the relationship between normalized compressive strength and SL replacement, which is visualized in Figure 9. The constants in Equation 3 were determined by curve-fitting the experimental compressive strength data for SL replacement levels of 0%, 20%, and 40%. The resulting prediction coefficient, $R^2 = 0.954$, indicates a high degree of correlation between the experimental data and the model, suggesting that the equation is reliable and suitable for practical engineering applications.

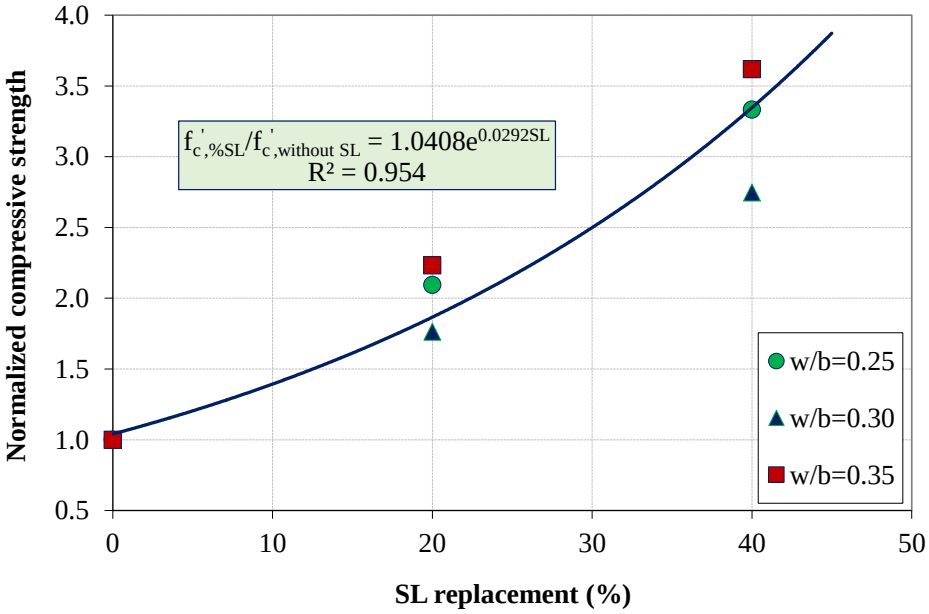

Figure 9. Normalization of compressive strength with SL replacement by the strength of one-part geopolymer mortar without SL as the divisor

Similarly, Figure 10 shows the normalized flexural strength for different SL replacement ratios, again using the flexural strength of one-part geopolymer mortar without SL as the baseline. The data from Figure 6 reveals a gradual improvement in flexural strength as the SL replacement ratio increased, alongside variations in the water-to-binder (w/b) ratio. Using the same curve-fitting process as applied to compressive strength, the constants for Equation 4 were determined using flexural strength data at SL replacement rates of 0%, 20%, and 40%. However, the prediction coefficient for the flexural strength model was $R^2 = 0.652$, which, while lower than that for compressive strength, still suggests a moderate correlation between the experimental data and the fitted Equation.

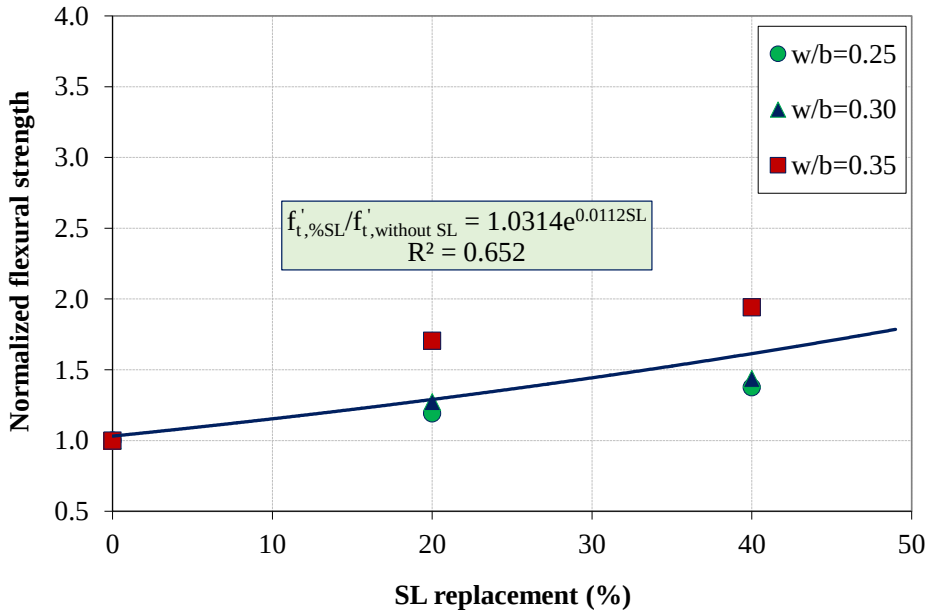

Figure 10. Normalization of flexural strength with SL replacement by the strength of one-part geopolymer mortar without SL as the divisor

$$\frac{f_{c,\%SL}}{f_{c,without\ SL}} = 1.0408e^{0.0292SL} \quad (3)$$

where $f_{c,\%SL}$ is the compressive strength at %SL replacement and $f_{c,without\ SL}$ is the compressive strength at 0% SL replacement.

$$\frac{f_{t,\%SL}}{f_{t,without\ SL}} = 1.0314e^{0.00112SL} \quad (4)$$

where $f_{t,\%SL}$ is the flexural strength at %SL replacement and $f_{t,without\ SL}$ is the flexural strength at 0% SL replacement.

Figure 7 illustrates the relationship between compressive strength and flexural strength of one-part geopolymer mortar, compared with previously published data on two-part geopolymer mortar and Portland cement (PC) mortar. This comparison is extended to the values recommended by ACI 318 [50] and AS 3600 [51]. Equation 5 represents the relationship suggested by ACI 318, while Equation 6 provides the corresponding relationship proposed by AS 3600. Based on the findings from this study, a simplified linear regression model was developed to describe the relationship between compressive strength and flexural strength of one-part geopolymer mortar, as shown in Equation 7. The prediction coefficient for this regression model, $R^2 = 0.835$, demonstrates a good level of reliability, indicating that the equation can be effectively used in engineering applications.

The results in Figure 11 reveal that the flexural strength of one-part geopolymer mortar increases linearly with the square root of its compressive strength. This finding aligns with the results from previous studies [52-55], which explored the behavior of two-part geopolymer mortars and PC mortars. Notably, the flexural strength values for geopolymer mortars are consistently higher than those predicted by the guidelines in ACI 318 [50] and AS 3600 [51]. This increase in flexural strength is attributed to the denser and stronger bond between the geopolymer paste and the aggregates, as previously reported by Sofi et al. [53] and Damrongwiriyanupap et al. [56]. The superior interfacial transition zone (ITZ) in geopolymer concrete leads to improved mechanical properties compared to conventional PC concrete.

$$f_t = 0.62\sqrt{f'_c} \quad (5)$$

$$f_t = 0.60\sqrt{f'_c} \quad (6)$$

$$f_t = 1.528\sqrt{f'_c} \quad (7)$$

where f_t is the flexural strength (MPa) and f'_c is the compressive strength (MPa).

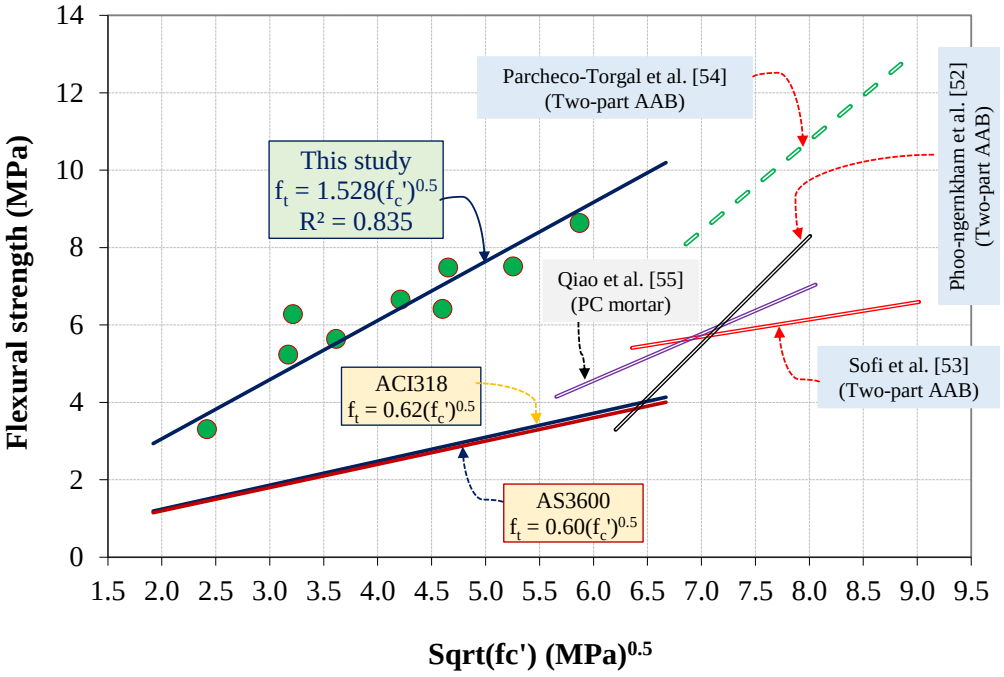

Figure 11. Relationship between compressive strength and flexural strength of one-part geopolymer mortar compared with previously published results of two-part geopolymer and PC mortars

3.5. Life Cycle Assessment (LCA)

As mentioned in Section 2.5, the scope of this LCA focuses solely on the production phase of one-part geopolymer materials, quantifying the environmental impacts primarily in terms of energy consumption and Global Warming Potential (GWP), expressed in kg of CO_2 equivalents. The transportation phase is excluded due to its variability based on location-specific factors such as transport distance, type of transportation, and storage methods. The LCA analysis was performed using the following steps:

3.5.1. Identification of Materials Used in Production

The key materials involved in the production of one-part geopolymer are:

- Fly Ash (FA)
- Sodium Silicate Powder (NP)
- Slag (SL)
- River Sand
- Tap Water

3.5.2. Environmental Impact Inventory Data

The environmental inventory data for each material used in this study was sourced from three references [57, 58, 59]. A detail summary of the Global Warming Potential (GWP) of each material is presented below:

- Fly Ash (FA): A byproduct of coal combustion, fly ash has a relatively low environmental impact compared to primary materials like cement. However, it requires some energy for transportation and minimal processing. GWP: 0.02 kg CO_2 -eq per kg of fly ash.
- Sodium Silicate Powder (NP): Sodium silicate is produced by combining sodium carbonate (soda ash) with silica (sand) at high temperatures in a furnace, making it one of the higher-impact materials in the mix. GWP: 1.00 kg CO_2 -eq per kg of sodium silicate powder.
- Slag (SL): Ground Granulated Blast Furnace Slag (GGBS) is a byproduct of steel production, with a lower carbon footprint than cement, yet still contributing significantly to the overall environmental impact. GWP: 0.08 kg CO_2 -eq per kg of slag.
- River Sand: River sand has a minor environmental impact in terms of CO_2 emissions, though its extraction can cause local environmental disruption. GWP: 0.005 kg CO_2 -eq per kg of river sand.
- Tap Water: The environmental impact of water used in construction is low, although energy is required for its extraction, pumping, and distribution. GWP: 0.0003 kg CO_2 -eq per kg of water.

3.5.3. Environmental Impact Inventory Data

Using the material inventory data and mix proportions provided, the total GWP of each geopolymer mix was calculated. The results are summarized in Table 3:

Table 3. GWP in terms of CO_2-equivalent

No.	Symbol	Total GWP (kg CO_2 -eq)
1	0.25/F9/N1/S0	109.33
2	0.25/F7/N1/S2	118.33
3	0.25/F5/N1/S4	127.35
4	0.30/F9/N1/S0	104.45
5	0.30/F7/N1/S2	114.03
6	0.30/F5/N1/S4	122.70
7	0.35/F9/N1/S0	100.62
8	0.35/F7/N1/S2	108.86
9	0.35/F5/N1/S4	118.17

Based on the LCA results, the following key findings are observed:

- *Water-to-Binder Ratio (w/b Ratio):*

The w/b ratio has a significant influence on the GWP of each mix. As the w/b ratio increases (from 0.25 to 0.35), the GWP consistently decreases. This reduction in GWP is attributed to the lower quantity of binder required at higher w/b ratios, as binders such as sodium silicate powder and slag are carbon-intensive materials.

- *Slag (SL) Content:*

Increasing the slag content (SL) results in higher GWP values across the mixes. Despite the relatively lower GWP of slag compared to other binders like cement, it still contributes significantly to the total emissions. The data shows that mixes with higher slag content (S4) exhibit increased GWP compared to those with lower slag content (S0 or S2).

- *Sodium Silicate Powder (NP):*

Sodium silicate powder has the highest GWP among all materials in the mix (1.00 kg CO_2-eq per kg). As the primary contributor to GWP in one-part geopolymer production, reducing the proportion of sodium silicate powder or finding alternative activators could substantially lower the overall carbon footprint.

- *Fly Ash (FA) Content:*

Fly ash has the lowest GWP (0.02 kg CO_2-eq per kg) among the binder materials used in the geopolymer mix. As a byproduct of coal combustion, it is an environmentally preferable material, contributing minimally to the overall GWP while providing essential material properties. Therefore, fly ash is an excellent candidate for use in sustainable geopolymer production.

- *Sand and Water:*

River sand and tap water contribute very little to the total GWP, with GWP values of 0.005 and 0.0003 kg CO□-eq per kg, respectively. Although used in significant quantities, their environmental impact is minor, accounting for less than 5% of the total GWP in most mixes.

3.5.4. Relationship between GWP and Compressive Strength

Using the GWP values obtained from 3.5.3 and the results on compressive strength, the relationship between GWP and compressive strength in terms of GWP per MPa for each mix can then be calculated and the results are shown in Table 4.

Table 4. GWP (kg CO_2 -eq) per Compressive Strength (MPa) for Each Mix

No.	Mix Symbol	Compressive Strength (MPa)	GWP (kg CO_2 -eq)	GWP per MPa (kg CO_2 -eq / MPa)
1	0.25/F9/N1/S0	10.3	109.3	10.61
2	0.30/F9/N1/S0	10.1	104.5	10.34
3	0.35/F9/N1/S0	5.9	100.6	17.05
4	0.25/F7/N1/S2	21.7	118.3	5.45
5	0.30/F7/N1/S2	17.7	114.0	6.44
6	0.35/F7/N1/S2	13.1	108.9	8.31
7	0.25/F5/N1/S4	34.5	127.4	3.69
8	0.30/F5/N1/S4	27.6	122.7	4.45
9	0.35/F5/N1/S4	21.2	118.2	5.57

3.5.4.1. Effect of Slag Content

In general, the results reveal that, although increasing the slag (SL) content in the geopolymer increases the overall GWP of the mixture, the GWP per MPa decreases significantly. This means that for every kilogram of CO_2 emitted, you achieve a higher compressive strength as slag content increases. For instance:

- 0.25/F5/N1/S4 (with 40% slag) has a compressive strength of 34.5 MPa and a GWP per MPa of 3.69 kg CO_2 -eq/MPa, the lowest in the entire study.
- Conversely, 0.35/F9/N1/S0 (with 0% slag) has a much lower compressive strength of 5.9 MPa, but a much higher GWP per MPa of 17.05 kg CO_2 -eq/MPa.

This clearly shows that higher slag content makes the geopolymer mixtures more environmentally efficient in terms of the strength achieved per unit of carbon emissions. The reduction in GWP per MPa as slag content increases suggests that slag improves the material's strength more efficiently than other components (such as fly ash or sodium silicate powder). Even though slag has a relatively higher GWP than fly ash, its strength-contributing properties justify its use from an environmental perspective.

3.5.4.2. Effect of Water-to-Binder (w/b) Ratio

Lower w/b ratios generally lead to higher compressive strengths, which also leads to a lower GWP per MPa. For instance, the mix 0.25/F5/N1/S4 (with a w/b ratio of 0.25 and 40% slag) has the best GWP per MPa. On the other hand, higher w/b ratios (like 0.35) result in reduced strength and higher GWP per MPa values. This suggests that keeping the w/b ratio low is crucial for optimizing both strength and environmental efficiency.

4. Conclusions

Based on the results of these experiments, the following conclusions can be drawn:

- Workability and Flowability: The workability and flowability of the one-part geopolymer mortar were significantly influenced by the slag (SL) replacement and water-to-binder (w/b) ratio. Mixtures with a higher w/b ratio exhibited higher relative slump values, improving flowability. However, increasing the SL replacement content generally reduced workability due to the higher water demand of slag and its angular particle shape.
- Setting Time: Lower w/b ratios and higher SL replacement resulted in a reduction in the setting time of the geopolymer paste. The higher calcium content from the slag (SL) accelerated the geopolymerization process, leading to shorter setting times compared to geopolymer pastes without SL. This shows that SL plays a key role in the early strength development of one-part geopolymer.
- Mechanical Properties: The use of SL in the production of one-part FA-based geopolymer mortar had a positive effect on both compressive and flexural strengths. The highest compressive and flexural strengths at 28 days were achieved with 40% SL replacement, reaching 34.5 MPa and 8.6 MPa, respectively. Conversely, an increase in the w/b ratio led to a reduction in both compressive and flexural strengths, highlighting the importance of maintaining a lower w/b ratio to maximize strength performance.
- Strength-Property Relationships: The strength development of one-part geopolymer mortar with varying SL replacement and w/b ratios could be modeled effectively using an exponential function. Additionally, the relationship between compressive strength and flexural strength of the geopolymer mortar was represented by a simplified linear regression model. The R^2 value of 0.835 from the curve fitting indicates a good level of reliability for these models in predicting mechanical performance in engineering applications.
- Global Warming Potential (GWP): While increasing the SL content contributed to a higher overall GWP due to the embodied carbon of slag, the positive impact on compressive strength justified the use of SL. The mix with the highest SL replacement (40%) exhibited the highest compressive strength but also a slightly higher GWP compared to mixes with lower SL content. This suggests that while the use of SL improves mechanical performance, its contribution to GWP needs to be carefully managed in sustainability-focused applications.
- GWP per MPa: When normalized by compressive strength, the GWP per MPa was significantly lower in mixes with higher SL content. For example, the mix with 40% SL replacement had a GWP per MPa of 3.69 kg CO_2-eq/MPa, compared to 17.05 kg CO_2-eq/MPa for the mix with no SL replacement. This indicates that slag not only improves strength but also enhances the environmental efficiency of the one-part geopolymer in terms of GWP per unit strength, making it a more sustainable option for high-strength applications.

5. Declarations

5.1. Author Contributions

Conceptualization D.I., P.S., and T.P.; methodology, D.I., P.S., and T.P.; validation, S.H., V.S., P.Ch., W.S., and Pr.C.; formal analysis, D.I., P.Ch., and H.Z.; investigation, D.I. and P.Ch.; resources, P.S.; data curation, D.I. and P.Ch.; writing—original draft preparation, P.S. and H.Z.; writing—review and editing, P.S., H.Z., and T.P.; visualization, P.S.; supervision, P.S., T.P., and Pr.C.; project administration, P.S.; funding acquisition, P.S. and T.P. All authors have read and agreed to the published version of the manuscript.

5.2. Data Availability Statement

The data presented in this study are available on request from the corresponding author.

5.3. Funding

- This research is funded by the National Science, Research and Innovation Fund (NSRF) and King Mongkut's University of Technology North Bangkok under contract no. KMUTNB-FF-68-B-05.
- Tanakorn Phoo-ngernkham would like to acknowledge financial support from NSRF via the Program Management Unit for Human Resources & Institutional Development, Research and Innovation [grant number B05F640178].).

5.4. Acknowledgements

The authors gratefully acknowledge support from Professor Hexin Zhang from Edinburgh Napier University, UK, for proofreading the manuscript. Additionally, appreciation is extended to the Science, Technology, and Research Institute (STRI) at KMUTNB for their support in funding acquisition.

5.5. Conflicts of Interest

The authors declare no conflict of interest.

6. References

[1] Davidovits, J. (1991). Geopolymers - Inorganic polymeric new materials. Journal of Thermal Analysis, 37(8), 1633–1656. doi:10.1007/BF01912193.

[2] Cong, P., & Cheng, Y. (2021). Advances in geopolymer materials: A comprehensive review. Journal of Traffic and Transportation Engineering (English Edition), 8(3), 283–314. doi:10.1016/j.jtte.2021.03.004.

[3] Pacheco-Torgal, F., Castro-Gomes, J., & Jalali, S. (2008). Alkali-activated binders: A review. Part 2. About materials and binders manufacture. Construction and Building Materials, 22(7), 1315–1322. doi:10.1016/j.conbuildmat.2007.03.019.

[4] Sinsiri, T., Phoo-ngernkham, T., Sata, V., & Chindaprasirt, P. (2012). The effects of replacement fly ash with diatomite in geopolymer mortar. Computers and Concrete, 9(6), 427–437. doi:10.12989/cac.2012.9.6.427.

[5] Duxson, P., Fernández-Jiménez, A., Provis, J. L., Lukey, G. C., Palomo, A., & van Deventer, J. S. J. (2006). Geopolymer technology: the current state of the art. Journal of Materials Science, 42(9), 2917–2933. doi:10.1007/s10853-006-0637-z.

[6] Sukontasukkul, P., Chindaprasirt, P., Pongsopha, P., Phoo-Ngernkham, T., Tangchirapat, W., & Banthia, N. (2020). Effect of fly ash/silica fume ratio and curing condition on mechanical properties of fiber-reinforced geopolymer. Journal of Sustainable Cement-Based Materials, 9(4), 218–232. doi:10.1080/21650373.2019.1709999.

[7] Suksiripattanapong, C., Krosoongnern, K., Thumrongvut, J., Sukontasukkul, P., Horpibulsuk, S., & Chindaprasirt, P. (2020). Properties of cellular lightweight high calcium bottom ash-portland cement geopolymer mortar. Case Studies in Construction Materials, 12. doi:10.1016/j.cscm.2020.e00337.

[8] Yoosuk, P., Suksiripattanapong, C., Sukontasukkul, P., & Chindaprasirt, P. (2021). Properties of polypropylene fiber reinforced cellular lightweight high calcium fly ash geopolymer mortar. Case Studies in Construction Materials, 15. doi:10.1016/j.cscm.2021.e00730.

[9] Xue, L., Zhang, Z., & Wang, H. (2021). Hydration mechanisms and durability of hybrid alkaline cements (HACs): A review. Construction and Building Materials, 266(121039). doi:10.1016/j.conbuildmat.2020.121039.

[10] Chindaprasirt, P., Sriopas, B., Phosri, P., Yoddumrong, P., Anantakarn, K., & Kroehong, W. (2022). Hybrid high calcium fly ash alkali-activated repair material for concrete exposed to sulfate environment. Journal of Building Engineering, 45, 103590. doi:10.1016/j.jobe.2021.103590.

[11] Detphan, S., Phiangphimai, C., Wachum, A., Hanjitsuwan, S., Phoo-Ngernkham, T., & Chindaprasirt, P. (2021). Strength development and thermal conductivity of pofa lightweight geopolymer concrete incorporating Fa and Pc. Engineering and Applied Science Research, 48(6), 718–723. doi:10.14456/easr.2021.73.

[12] Phoo-ngernkham, T., Hanjitsuwan, S., Detphan, S., Thumrongvut, J., Suksiripattanapong, C., Damrongwiriyanupap, N., Chindaprasirt, P., & Hatanaka, S. (2018). Shear bond strength of FA-PC geopoylmer under different sand to binder ratios and sodium hydroxide concentrations. International Journal of GEOMATE, 14(42), 52–57. doi:10.21660/2018.42.7152.

[13] Omulepu, O., & Bryan, D. J. (2010). Chapter 100 - Chemical Injuries. Plastic Surgery Secrets Plus (Second Edition), Mosby, Missouri, United States. doi:10.1016/B978-0-323-03470-8.X0001-4.

[14] Zhang, H. Y., Liu, J. C., & Wu, B. (2021). Mechanical properties and reaction mechanism of one-part geopolymer mortars. Construction and Building Materials, 273, 121973. doi:10.1016/j.conbuildmat.2020.121973.

[15] Tesanasin, T., Suksiripattanapong, C., Van Duc, B., Tabyang, W., Phetchuay, C., Phoo-ngernkham, T., Sukontasukkul, P., & Chindaprasirt, P. (2022). Engineering properties of marginal lateritic soil stabilized with one-part high calcium fly ash geopolymer as pavement materials. Case Studies in Construction Materials, 17. doi:10.1016/j.cscm.2022.e01328.

[16] Phiangphimai, C., Joinok, G., Phoo-ngernkham, T., Damrongwiriyanupap, N., Hanjitsuwan, S., Suksiripattanapong, C., Sukontasukkul, P., & Chindaprasirt, P. (2023). Durability properties of novel coating material produced by alkali-activated/cement powder. Construction and Building Materials, 363, 129837. doi:10.1016/j.conbuildmat.2022.129837.

[17] Phiangphimai, C., Joinok, G., Phoo-ngernkham, T., Hanjitsuwan, S., Damrongwiriyanupap, N., Sae-Long, W., Sukontasukkul, P., & Chindaprasirt, P. (2023). Shrinkage, compressive and bond strengths of alkali activated/cement powder for alternative coating applications. Construction and Building Materials, 400, 132631. doi:10.1016/j.conbuildmat.2023.132631.

[18] Kogbara, R. B., Al-Zubi, A., Mortada, Y., Hammoud, A., Masad, E. A., & Khraisheh, M. K. (2024). Lime-activated one-part geopolymer mortars from construction, demolition and industrial wastes. Results in Engineering, 21(101739). doi:10.1016/j.rineng.2023.101739.

[19] Intarabut, D., Sukontasukkul, P., Phoo-Ngernkham, T., Zhang, H., Yoo, D. Y., Limkatanyu, S., & Chindaprasirt, P. (2022). Influence of Graphene Oxide Nanoparticles on Bond-Slip Reponses between Fiber and Geopolymer Mortar. Nanomaterials, 12(6), 943. doi:10.3390/nano12060943.

[20] Liew, Y. M., Heah, C. Y., Li, L. yuan, Jaya, N. A., Abdullah, M. M. A. B., Tan, S. J., & Hussin, K. (2017). Formation of one-part-mixing geopolymers and geopolymer ceramics from geopolymer powder. Construction and Building Materials, 156, 9–18. doi:10.1016/j.conbuildmat.2017.08.110.

[21] Feng, D., Provis, J. L., & Van Deventer, J. S. J. (2012). Thermal activation of albite for the synthesis of one-part mix geopolymers. Journal of the American Ceramic Society, 95(2), 565–572. doi:10.1111/j.1551-2916.2011.04925.x.

[22] Hajimohammadi, A., & van Deventer, J. S. J. (2017). Characterisation of One-Part Geopolymer Binders Made from Fly Ash. Waste and Biomass Valorization, 8(1), 225–233. doi:10.1007/s12649-016-9582-5.

[23] Sturm, P., Gluth, G. J. G., Simon, S., Brouwers, H. J. H., & Kühne, H. C. (2016). The effect of heat treatment on the mechanical and structural properties of one-part geopolymer-zeolite composites. Thermochimica Acta, 635, 41–58. doi:10.1016/j.tca.2016.04.015.

[24] Mohammed, B. S., Haruna, S., Wahab, M. M. A., Liew, M. S., & Haruna, A. (2019). Mechanical and microstructural properties of high calcium fly ash one-part geopolymer cement made with granular activator. Heliyon, 5(9), e02255. doi:10.1016/j.heliyon.2019.e02255.

[25] Nematollahi, B., Sanjayan, J., & Shaikh, F. U. A. (2015). Synthesis of heat and ambient cured one-part geopolymer mixes with different grades of sodium silicate. Ceramics International, 41(4), 5696–5704. doi:10.1016/j.ceramint.2014.12.154.

[26] Maho, B., Sukontasukkul, P., Sua-Iam, G., Sappakittipakorn, M., Intarabut, D., Suksiripattanapong, C., Chindaprasirt, P., & Limkatanyu, S. (2021). Mechanical properties and electrical resistivity of multiwall carbon nanotubes incorporated into high calcium fly ash geopolymer. Case Studies in Construction Materials, 15, e00785. doi:10.1016/j.cscm.2021.e00785.

[27] Phoo-Ngernkham, T., Maegawa, A., Mishima, N., Hatanaka, S., & Chindaprasirt, P. (2015). Effects of sodium hydroxide and sodium silicate solutions on compressive and shear bond strengths of FA-GBFS geopolymer. Construction and Building Materials, 91(0), 1–8. doi:10.1016/j.conbuildmat.2015.05.001.

[28] Sukontasukkul, P., Intarabut, D., Phoo-ngernkham, T., Suksiripattanapong, C., Zhang, H., & Chindaprasirt, P. (2023). Self-compacting steel fibers reinforced geopolymer: Study on mechanical properties and durability against acid and chloride attacks. Case Studies in Construction Materials, 19. doi:10.1016/j.cscm.2023.e02298.

[29] Zheng, Z., & Deng, P. (2024). Mechanical and fracture properties of slag/steel slag-based geopolymer fully recycled aggregate concrete. Construction and Building Materials, 413(134533). doi:10.1016/j.conbuildmat.2023.134533.

[30] Dueramae, S., Tangchirapat, W., Sukontasukkul, P., Chindaprasirt, P., & Jaturapitakkul, C. (2019). Investigation of compressive strength and microstructures of activated cement free binder from fly ash-calcium carbide residue mixture. Journal of Materials Research and Technology, 8(5), 4757–4765. doi:10.1016/j.jmrt.2019.08.022.

[31] Yousefi Oderji, S., Chen, B., Ahmad, M. R., & Shah, S. F. A. (2019). Fresh and hardened properties of one-part fly ash-based geopolymer binders cured at room temperature: Effect of slag and alkali activators. Journal of Cleaner Production, 225, 1–10. doi:10.1016/j.jclepro.2019.03.290.

[32] Chen, C., Shenoy, S., Pan, Y., Sasaki, K., Tian, Q., & Zhang, H. (2024). Mechanical activation of coal gasification slag for one-part geopolymer synthesis by alkali fusion and component additive method. Construction and Building Materials, 411, 134585. doi:10.1016/j.conbuildmat.2023.134585.

[33] ASTM C618-22 (2023). Standard Specification for Coal Fly Ash and Raw or Calcined Natural Pozzolan for Use in Concrete. ASTM International, Pennsylvania, United States. doi:10.1520/C0618-22

[34] Sarıdemir, M., & Çelikten, S. (2023). Effects of MS modulus, NA concentration and fly ash content on properties of vapour-cured geopolymer mortars exposed to high temperatures. Construction and Building Materials, 363, 129868. doi:10.1016/j.conbuildmat.2022.129868.

[35] Humad, A. M., Kothari, A., Provis, J. L., & Cwirzen, A. (2019). The effect of blast furnace slag/fly ash ratio on setting, strength, and shrinkage of alkali-activated pastes and concretes. Frontiers in Materials, 6. doi:10.3389/fmats.2019.00009.

[36] ASTM C191-13. (2018). Standard Test Methods for Time of Setting of Hydraulic Cement by Vicat Needle Standard Test Methods for Time of Setting of Hydraulic Cement by Vicat Needle. ASTM International, Pennsylvania, United States. doi:10.1520/C0191-13.

[37] ASTM C109/C109M-20. (2020). Standard test method of compressive strength of hydraulic cement mortars (using 2-in. or [50 mm] cube speciments). ASTM International, Pennsylvania, United States. doi:10.1520/C0109_C0109M-20.

[38] ASTM C348-21. (2021). Standard Test Method for Flexural Strength of Hydraulic-Cement Mortars. ASTM International, Pennsylvania, United States. doi:10.1520/C0348-21.

[39] Lee, N. K., & Lee, H. K. (2013). Setting and mechanical properties of alkali-activated fly ash/slag concrete manufactured at room temperature. Construction and Building Materials, 47(0), 1201–1209. doi:10.1016/j.conbuildmat.2013.05.107.

[40] Temuujin, J., van Riessen, A., & Williams, R. (2009). Influence of calcium compounds on the mechanical properties of fly ash geopolymer pastes. Journal of Hazardous Materials, 167(1–3), 82–88. doi:10.1016/j.jhazmat.2008.12.121.

[41] Damrongwiriyanupap, N., Wongchairattana, S., Phoo-Ngernkham, T., Petcherdchoo, A., Limkatanyu, S., & Chindaprasirt, P. (2023). Influence of Recycled Glass on Strength Development of Alkali-Activated High-Calcium Fly Ash Mortar. Advances in Materials Science and Engineering, 9418619. doi:10.1155/2023/9418619.

[42] Chindaprasirt, P., Phoo-ngernkham, T., Hanjitsuwan, S., Horpibulsuk, S., Poowancum, A., & Injorhor, B. (2018). Effect of calcium-rich compounds on setting time and strength development of alkali-activated fly ash cured at ambient temperature. Case Studies in Construction Materials, 9. doi:10.1016/j.cscm.2018.e00198.

[43] Vikas, G., & Rao, T. D. G. (2021). Setting Time, Workability and Strength Properties of Alkali Activated Fly Ash and Slag Based Geopolymer Concrete Activated with High Silica Modulus Water Glass. Iranian Journal of Science and Technology - Transactions of Civil Engineering, 45(3), 1483–1492. doi:10.1007/s40996-021-00598-8.

[44] Perná, I., & Hanzlíček, T. (2016). The setting time of a clay-slag geopolymer matrix: The influence of blast-furnace-slag addition and the mixing method. Journal of Cleaner Production, 112, 1150–1155. doi:10.1016/j.jclepro.2015.05.069.

[45] Phoo-ngernkham, T., Hanjitsuwan, S., Li, L., Damrongwiriyanupap, N., & Chindaprasirt, P. (2019). Adhesion characterisation of Portland cement concrete and alkali-activated binders. Advances in Cement Research, 31(2), 69–79. doi:10.1680/jadcr.17.00122.

[46] Guo, X., Shi, H., Chen, L., & Dick, W. A. (2010). Alkali-activated complex binders from class C fly ash and Ca-containing admixtures. Journal of Hazardous Materials, 173(1–3), 480–486. doi:10.1016/j.jhazmat.2009.08.110.

[47] Yip, C. K., Lukey, G. C., & van Deventer Dean, J. S. J. (2006). Effect of Blast Furnace Slag Addition on Microstructure and Properties of Metakaolinite Geopolymeric Materials. Advances in Ceramic Matrix Composites IX, the American Ceramic Society, Ohio, United States. doi:10.1002/9781118406892.ch13.

[48] Pacheco-Torgal, F. (2015). Introduction to Handbook of Alkali-activated Cements, Mortars and Concretes. Handbook of Alkali-Activated Cements, Mortars and Concretes, Woodhead Publishing, Sawston, United Kingdom. doi:10.1533/9781782422884.1.

[49] Rao, G. A. (2001). Generalization of Abrams' law for cement mortars. Cement and Concrete Research, 31(3), 495–502. doi:10.1016/S0008-8846(00)00473-7.

[50] ACI 318-14. (2014). Building Code Requirements for Structural Concrete (ACI 318-14) and Commentary (318R-14). American Concrete Institute (ACI), Michigan, United States.

[51] AS 3600-2009. (2009). Concrete structures Australian Standards, Sydney, Australia.

[52] Phoo-ngernkham, T., Sata, V., Hanjitsuwan, S., Ridtirud, C., Hatanaka, S., & Chindaprasirt, P. (2016). Compressive strength, Bending and Fracture Characteristics of High Calcium Fly Ash Geopolymer Mortar Containing Portland Cement Cured at Ambient Temperature. Arabian Journal for Science and Engineering, 41(4), 1263–1271. doi:10.1007/s13369-015-1906-4.

[53] Sofi, M., van Deventer, J. S. J., Mendis, P. A., & Lukey, G. C. (2007). Engineering properties of inorganic polymer concretes (IPCs). Cement and Concrete Research, 37(2), 251–257. doi:10.1016/j.cemconres.2006.10.008.

[54] Pacheco-Torgal, F., Castro-Gomes, J. P., & Jalali, S. (2008). Adhesion characterization of tungsten mine waste geopolymeric binder. Influence of OPC concrete substrate surface treatment. Construction and Building Materials, 22(3), 154–161. doi:10.1016/j.conbuildmat.2006.10.005.

[55] Qiao, F., Chau, C. K., & Li, Z. (2010). Property evaluation of magnesium phosphate cement mortar as patch repair material. Construction and Building Materials, 24(5), 695–700. doi:10.1016/j.conbuildmat.2009.10.039.

[56] Damrongwiriyanupap, N., Srikhamma, T., Plongkrathok, C., Phoo-ngernkham, T., Sae-Long, W., Hanjitsuwan, S., Sukontasukkul, P., Li, L. yuan, & Chindaprasirt, P. (2022). Assessment of equivalent substrate stiffness and mechanical properties of sustainable alkali-activated concrete containing recycled concrete aggregate. Case Studies in Construction Materials, 16. doi:10.1016/j.cscm.2022.e00982.

[57] Hammond, G., & Jones, C. (2008). Inventory of carbon & energy: ICE (Vol. 5). Sustainable Energy Research Team, Department of Mechanical Engineering, University of Bath, Bath, United Kingdom.

[58] Ecoinvent. (2018). Ecoinvent. Ecoinvent Database (Version 3.8). Swiss Centre for Life Cycle Inventories. Available online: https://www.ecoinvent.org/ (accessed on November 2024).

[59] WRAP. (2012). Environmental benefits of recycling – Aggregates case study. Waste & Resources Action Programme (WRAP), London, United Kingdom.